EUROPEAN UNION
European Structural and Investment Funds
Operational Programme Research,
Development and Education

FZU Institute of Physics of the Czech Academy of Sciences

Optical spectroscopy and biosensors for investigation of biomolecules and their interactions

Jakub Dostalek

AIT - Austrian Institute of Technology GmbH
Biosensor Technologies Unit
Konrad-Lorenz-Strasse 24 | 3430 Tulln | Austria
T +43(0) 664 2351773

FZU – Institute of Physics of the Czech Academy of Sciences,
Na Slovance 1 | Prague 182 00 | Czech Republic
T+420 776767927

jakub.dostalek@ait.ac.at | http://www.ait.ac.at | http://www.jakubdostalek.cz

Affinity Reactions on Surfaces and Assay Types

Content

- Spatially controlled functionalization
- Langmuir model, models for diffusion mass transfer - limited reaction.
- Microfluidics in affinity-based sensors.
- Formats used for affinity assays. Direct and indirect immunoassays and their characteristics.

Spatially Controlled Functionalization

Contact Spotting

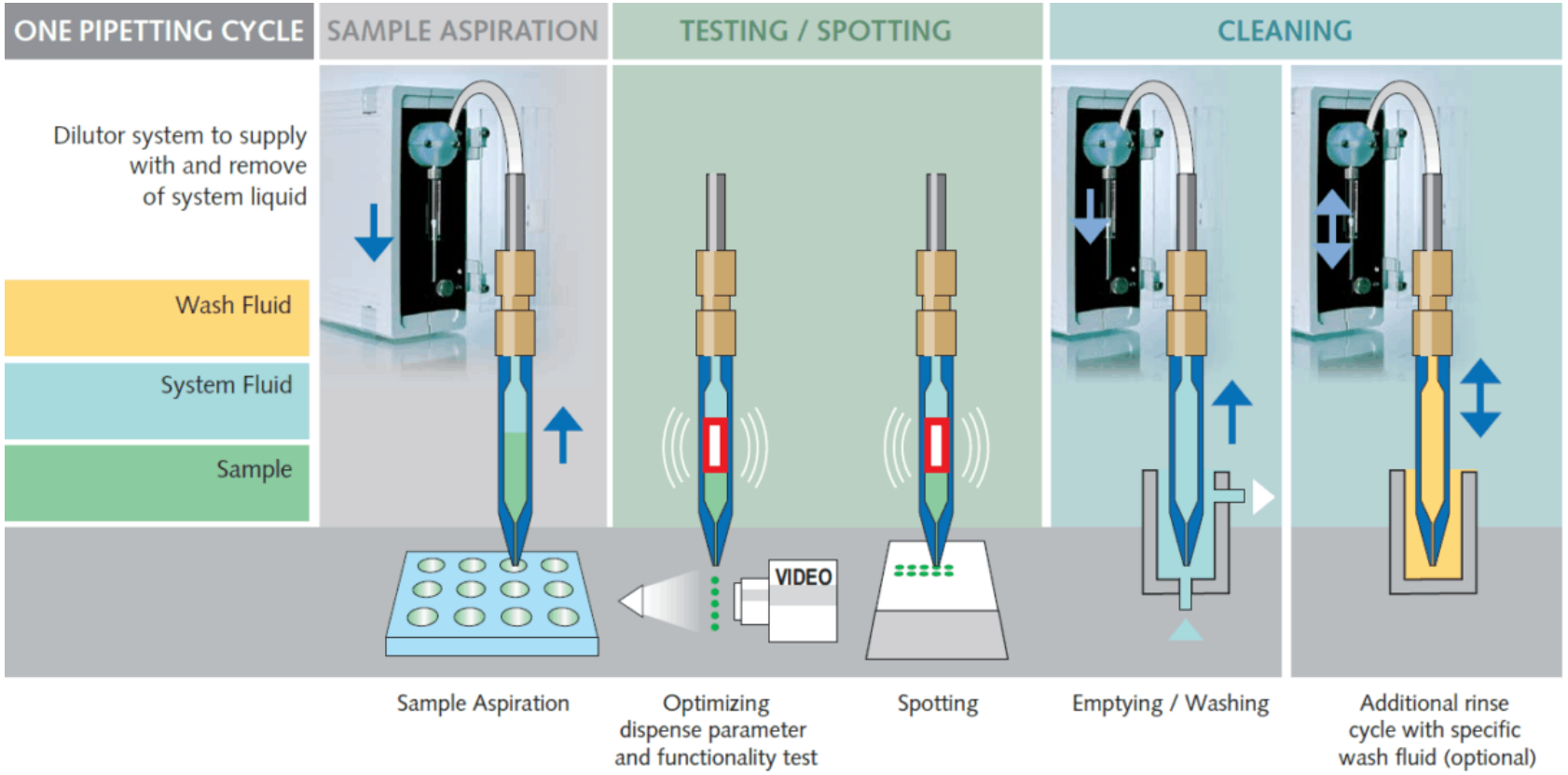

https://gesim-bioinstruments-microfluidics.com/microarray-printer/

Typical spot size of 100 µm.

Soft Lithography

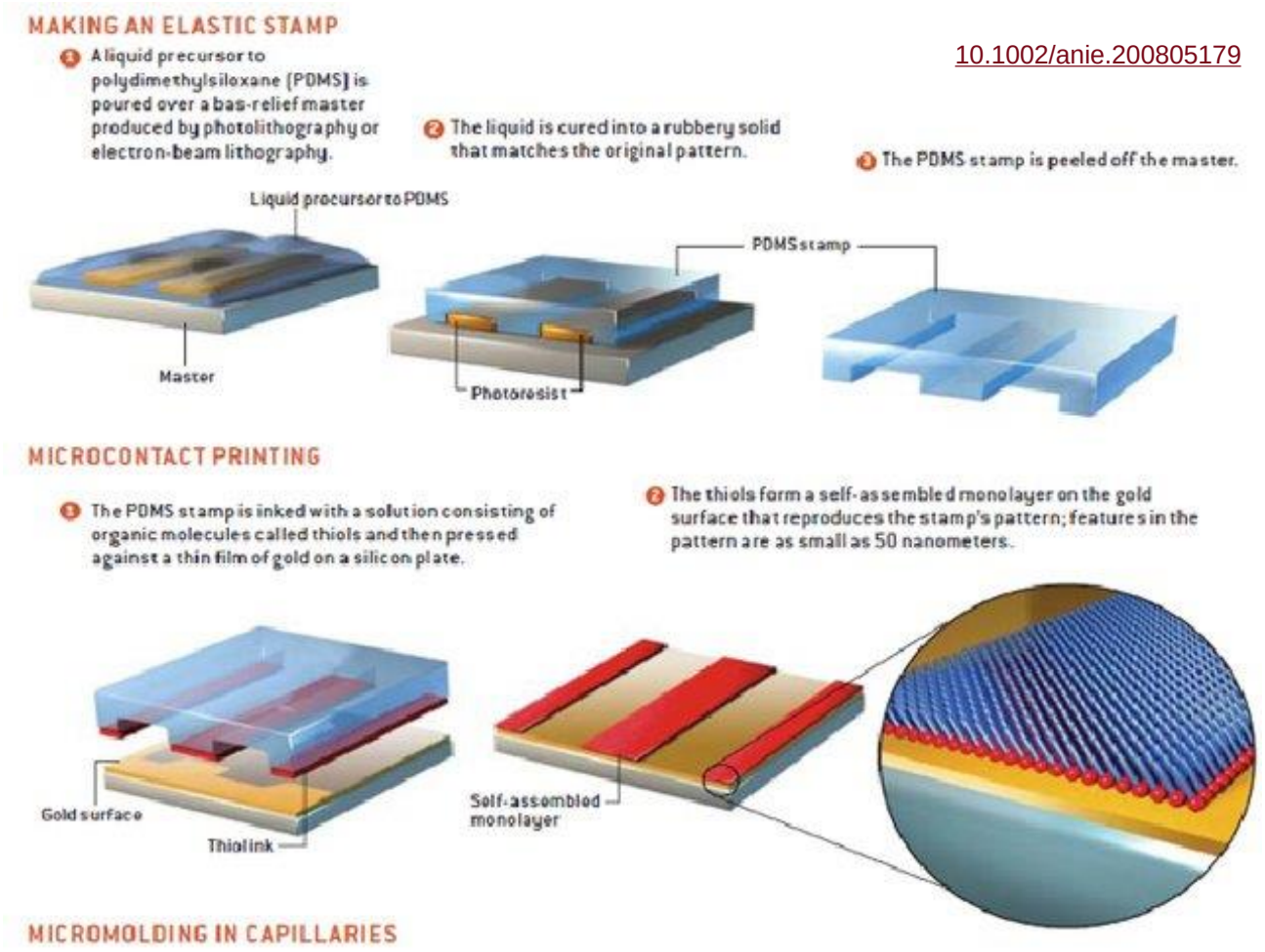

10.1002/anie.200805179

Nano-Fountain / Dip Pen Nanolithography

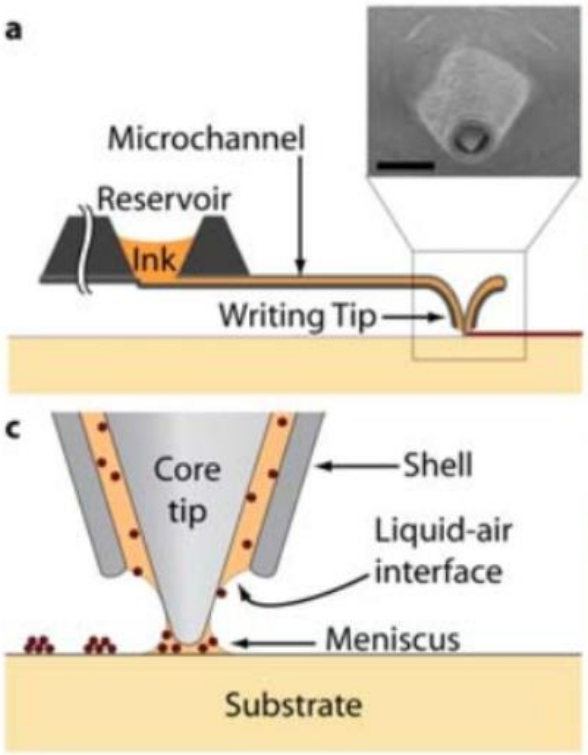

•10.1109/INEC.2010.5424494

Fluorescence AFM

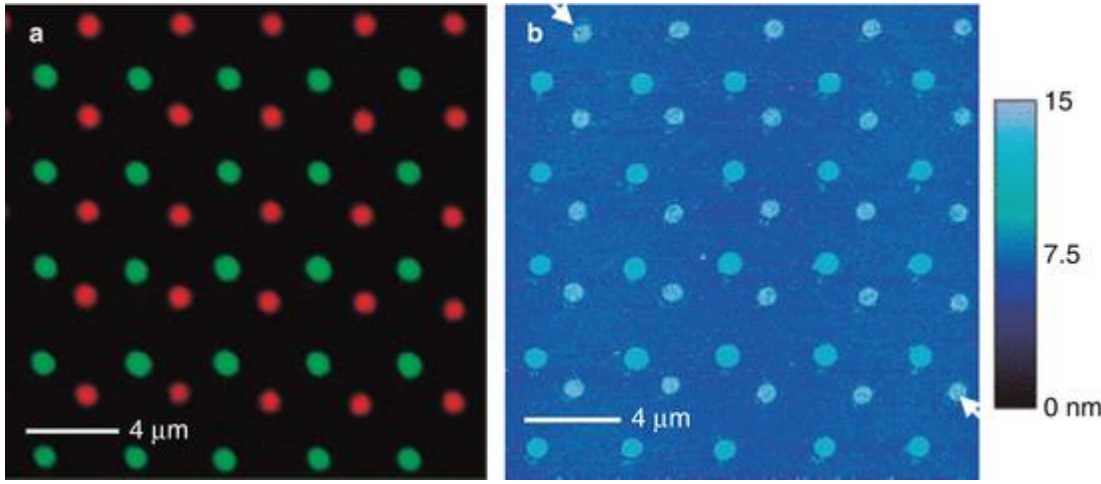

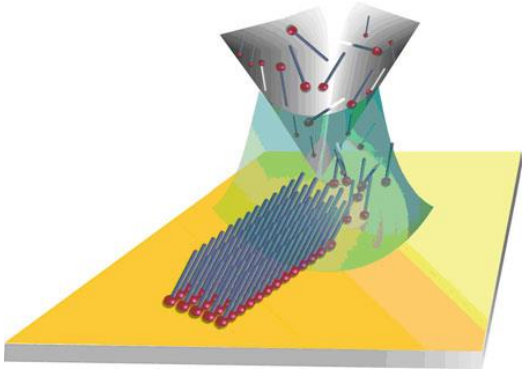

Demers, L.M., Ginger, D.S., Park, S.J., Li, Z., Chung, S.W., Mirkin, C.A.: Direct patterning of modified oligonucleotides on metals and insulators by dip-pen nanolithography. Science 296, 1836–1838 (2002)

https://doi.org/10.1007/978-90-481-9751-4_282

EUROPEAN UNION
European Structural and Investment Funds
Operational Programme Research,
Development and Education

MINISTRY OF EDUCATION, YOUTH AND SPORTS

FZU Institute of Physics of the Czech Academy of Sciences

AIT AUSTRIAN INSTITUTE OF TECHNOLOGY

Microfluidics – based Functionalization

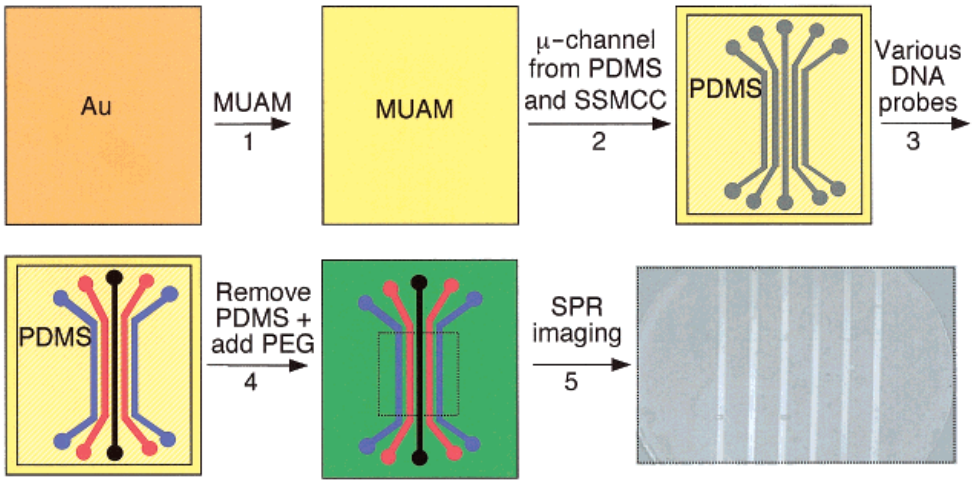

10.1021/ac010762s

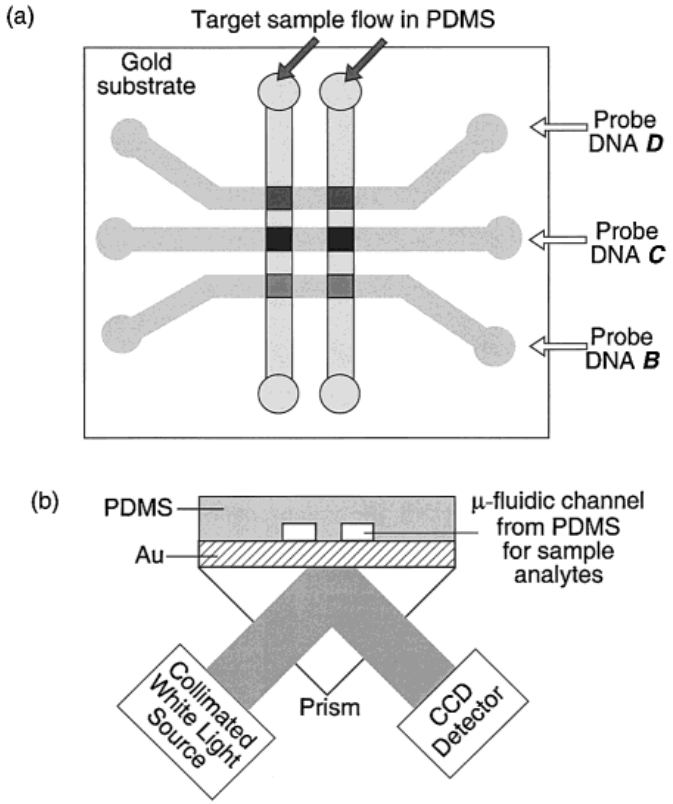

- Spatially controlled delivery of reagents by flow channels contacted with the surface.

Diffusion Mass Transfer-Limited Reaction Kinetics

EUROPEAN UNION
European Structural and Investment Funds
Operational Programme Research,
Development and Education

MINISTRY OF EDUCATION,
YOUTH AND SPORTS

FZU Institute of Physics of the Czech Academy of Sciences

AIT AUSTRIAN INSTITUTE OF TECHNOLOGY

Langmuir Adsorption Isotherm: Assumptions

- All adsorption sites identical
- Adsorbed species interact only with adsorptions sites, not with each other
- Adsorption limited to a monolayer

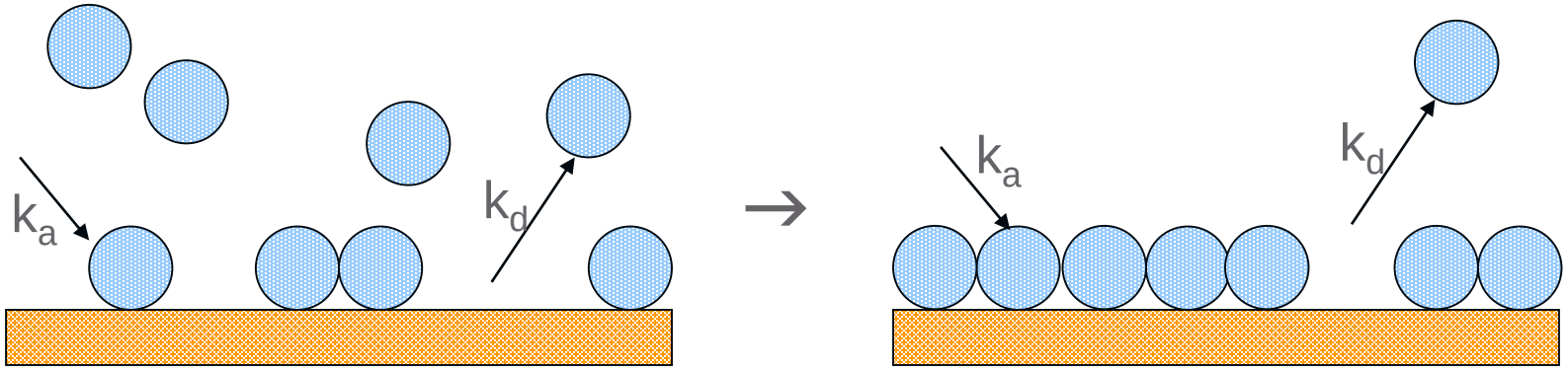

Langmuir Adsorption Isotherm

Equilibrium of a reaction:

$$A + B \underset{k_d}{\overset{k_a}{\rightleftarrows}} AB \qquad K = \frac{k_a}{k_d}$$

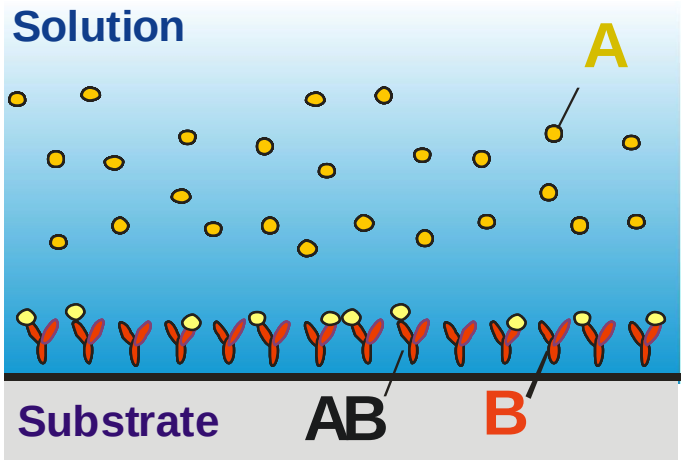

Kinetics of the reaction on a surface:

$$\frac{d\gamma}{dt} = k_a \alpha_0 (\beta - \gamma) - k_d \gamma$$

γ Concentration of [AB]

α_0 Concentration [A]

β Concentration [B]

Describes the interaction for:

a) Identical monovalent receptors B
b) Constant concentration of A in the solution ([A]>>[B])

(Possible to describe more complicated interactions e.g. multivalent receptors)

Two Compartment Model

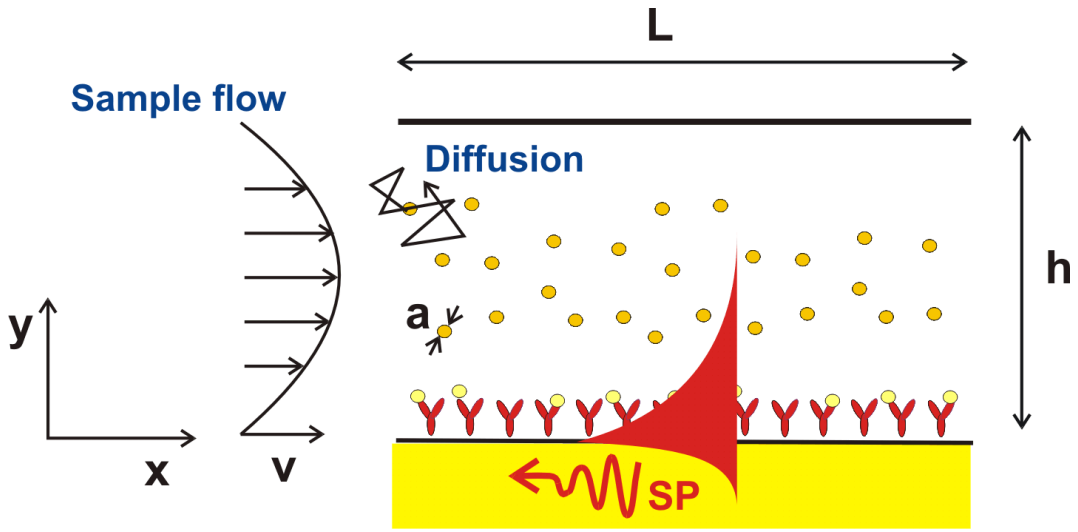

D – diffusion coefficient

$$D \approx \frac{k_B T}{6\pi a \eta}$$

a – molecule A hydrodynamic radius

η - solution viscosity

In SPR biosensors, analyte molecules A in a liquid samples are flowed over the sensor surface.

Due to the friction, at the surface the flow velocity is *v*=0. Approximation that the analyte mass transfer rate occurs across an unstirred layer through diffusion:

$$k_m = \xi \left(\frac{v_{\max} D^2}{hL} \right)^{1/3}$$

Full Model

A) Description of laminar flow and diffusion in a flow-cell

$$\frac{\partial \alpha(x,y,t)}{\partial t} = D\left(\frac{\partial^2 \alpha(x,y,t)}{\partial^2 x} + \frac{\partial^2 \alpha(x,y,t)}{\partial^2 y}\right) - 4v_{\max}\frac{y}{h}\left(1-\frac{y}{h}\right)\frac{\partial \alpha(x,y,t)}{\partial x}$$

B) Binding to receptors on the flow-cell bottom

$$\frac{\partial \gamma(x,t)}{\partial t} = k_a \alpha(x,0,t)\left[\beta - \gamma(x,t)\right] - k_d \gamma(x,t)$$

C) Boundary conditions :

$$D\frac{\partial \alpha(x,h,t)}{\partial y} = 0 \qquad D\frac{\partial \alpha(x,0,t)}{\partial y} = \frac{\partial \gamma(x,t)}{\partial t}$$

Mass Transport Limited Kinetics

„Corrected Langmuir equation“:

$$\frac{d\langle\gamma\rangle}{dt} = k_a^{eff}\,\alpha_0\left(\beta - \langle\gamma\rangle\right) - k_d^{eff}\,\langle\gamma\rangle$$

Valid when the diffusion parallel the sensor surface can be omitted (diffusion is much slower than the flow through the flow-cell)

$$k_a^{eff} = \frac{k_a}{1 + k_a\left[\beta - \langle\gamma\rangle(t)\right]/k_M}$$

$$k_d^{eff} = \frac{k_d}{1 + k_a\left[\beta - \langle\gamma\rangle(t)\right]/k_M}$$

$$\mathrm{Pe} = \frac{v_{\max} h^2}{DL} >> 1$$

$$k_M \approx 1.378\left(\frac{v_{\max} D^2}{hL}\right)^{1/3}$$

Mass transport can be omitted when Damköhler number Da<<1:

$$\mathrm{Da} = k_a \beta \left(\frac{v_{\max} D^2}{hL}\right)^{-1/3} << 1 \quad \Rightarrow \quad k_a^{eff} \approx k_a \quad k_d^{eff} \approx k_d$$

J. Stepanek et al. in J. Homola (Ed.), Surface Plasmon Resonance Based Sensors, Springer (2006) 45-69.

Surface Reaction with Mass Transfer

Reaction kinetics become a function of mass transfer rate k_m.

$$\frac{d\gamma}{dt} = k_{on}\alpha(\beta-\gamma) - k_{off}\gamma$$

$$k_{on} = \frac{k_a}{1 + k_a\left[\beta - \gamma(t)\right]/k_m}$$

$$k_{off} = \frac{k_d}{1 + k_a\left[\beta - \gamma(t)\right]/k_m}$$

Fast diffusion

$k_m >> k_a\beta$

Reaction is affinity-controlled and $k_{on} \approx k_a$, $k_{off} \approx k_d$

Slow diffusion

$k_m << k_a\beta$

Reaction is diffusion-controlled, $k_{on} \approx k_m\beta^{-1}$ and $k_{off} \approx k_m k_d (k_a\beta)^{-1}$

(low probe / ligand density, high flow rate)

EUROPEAN UNION
European Structural and Investment Funds
Operational Programme Research, Development and Education
MINISTRY OF EDUCATION, YOUTH AND SPORTS
FZU Institute of Physics of the Czech Academy of Sciences
AIT AUSTRIAN INSTITUTE OF TECHNOLOGY

Typical Characteristics

Properties of biomolecules:

Affinity constants: $k_a=10^{3}$-10^{7} $M^{-1}s^{-1}$ and $k_d=10^{-4}$-0.1 s^{-1} for majority of protein-protein interactions.

Diffusion constant: $D=2.4\times10^{-7}$ cm^2s^{-1} for water, T=20 ºC and a molecule with the diameter a=10 nm.

Fluidic system parameters:

Flow-rate: θ=100 µL/min

Flow-cell parameters: width *w*=5mm, height *h*=0.5mm, length *L*=10mm

Peclé number: Pe~400 (>>1 needed)

Damköhler number: Da~10^{-3} (<<1 needed) for β=10 ng mm^2, MW=160 kDa, $k_a=10^{7}$ M^{-1}s-1, $D=2.4\times10^{-5}$ mm^2s^{-1}, h=0.5 mm, Pe=400

Fitting of the Sensor Kinetics

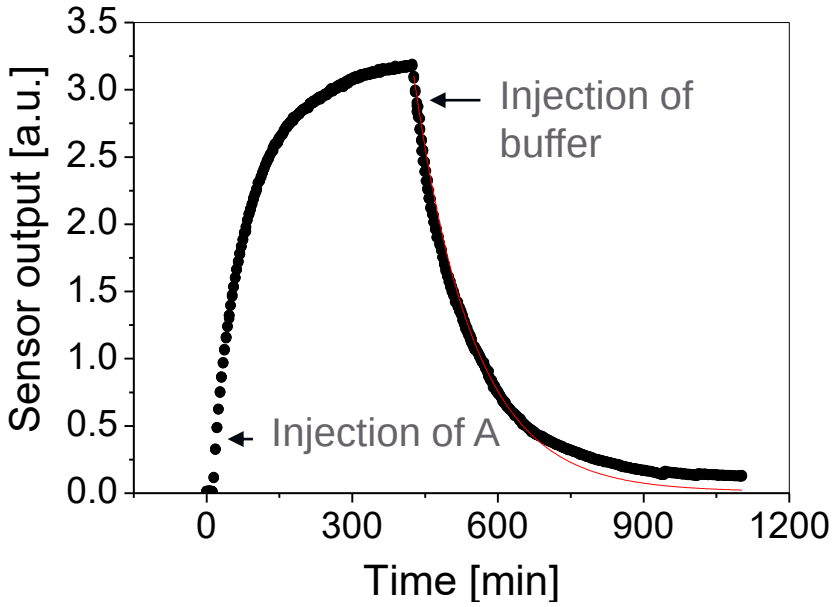

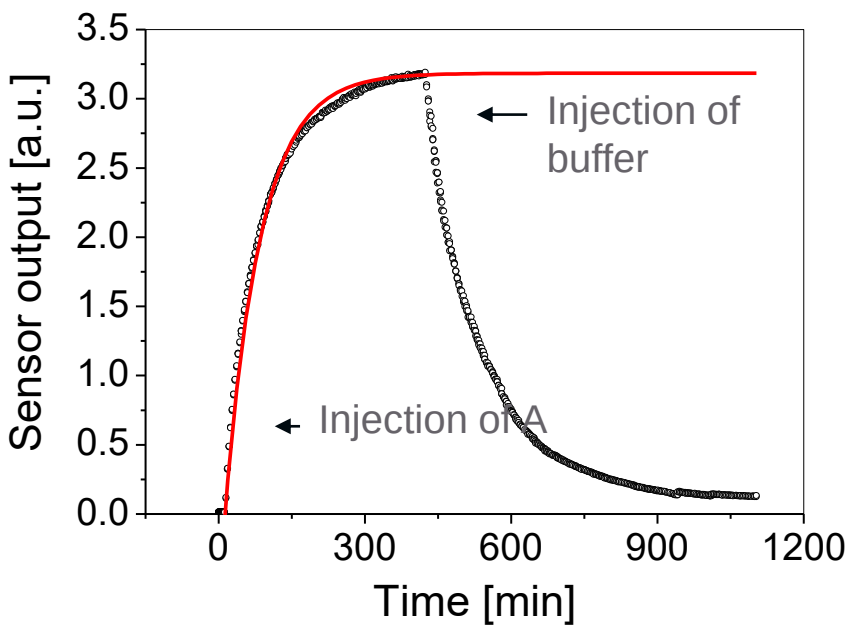

SPR biosensor output R(t) is proportional to $\gamma(t)$, one can fit k_a and k_d as:

$$R_d(t) = (R_{max} - R_0)e^{-k_d(t-t_a)} + R_0 \qquad R_a(t) = (R_{max} - R_0)(1 - e^{-(k_a c_0 - k_d)(t-t_0)}) + R_0$$

k_d! k_a!

Example – DNA Hybridization

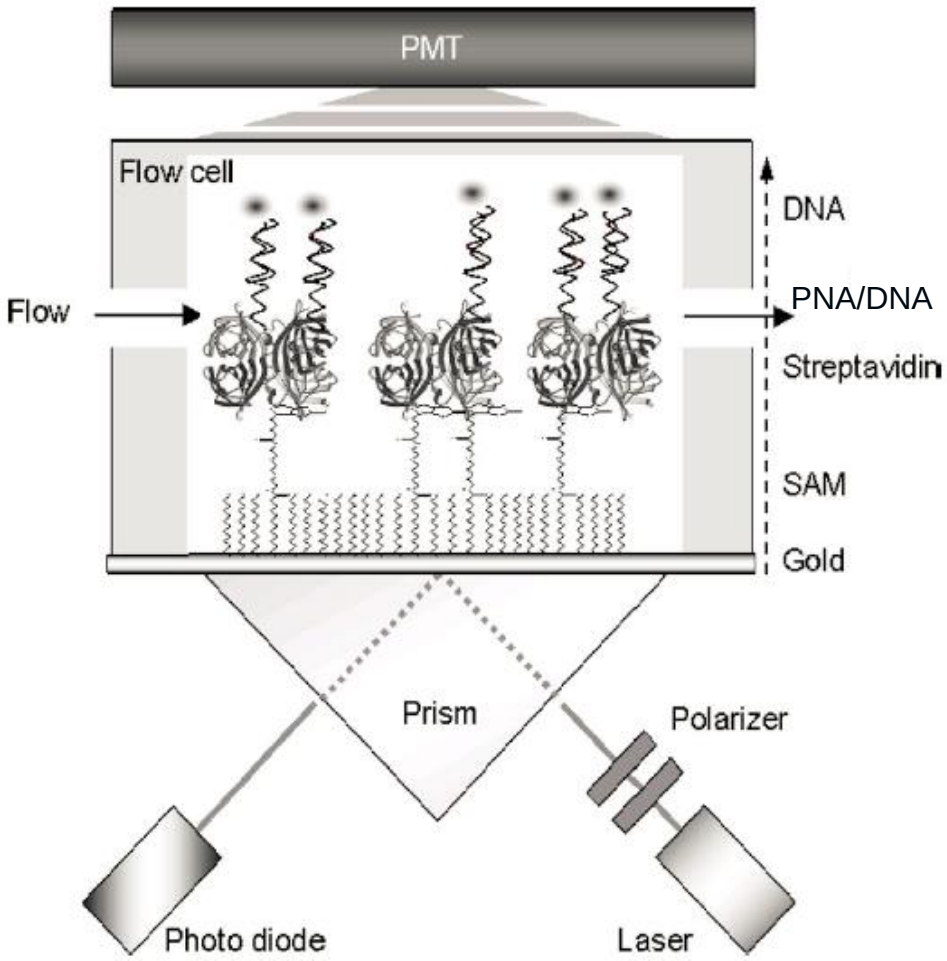

Example: investigation of peptide nucleic acid (PNA) probes for the detection of single nucleotide polymorphism (SNP).

- Relevant to e.g. diagnosis of genetic diseases such as thalassemia.
- Instrumentation: combined SPR and surface plasmon-enhanced fluorescence spectroscopy (SPFS).

H. Park, A. Germini, S. Sforza, R. Corradini, R. Marchelli, and Knoll W. ,BioInterphases **1, 113 2006.**

DNA Hybridization – Number of Bases

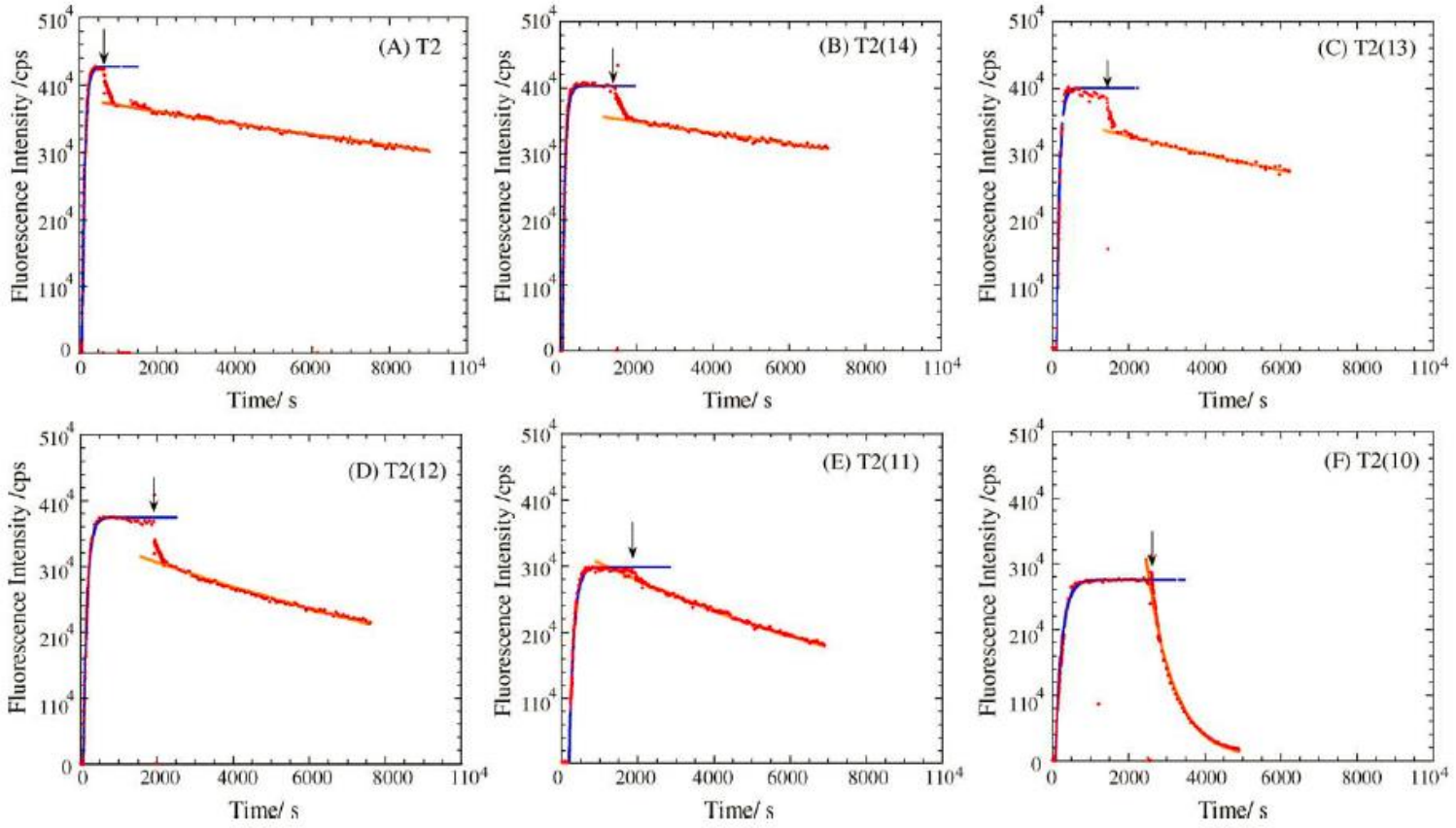

DNA probe: 5′-biotin-TTT TTT TTT TTT TTT TGT ACA TCA CAA CTA-3′

DNA targets:

T2: 3′-ACA TGT AGT GTT GAT-Cy5-5′

T2(14): 3′-CA TGT AGT GTT GAT-Cy5-5′

…

T2(10): 3′-T AGT GTT GAT-Cy5-5′

K. Tawa, D. F. Yao, and W. Knoll, Biosens. Bioelectron. **21, 322 2005.**

DNA Hybridization: Mismatch Detection

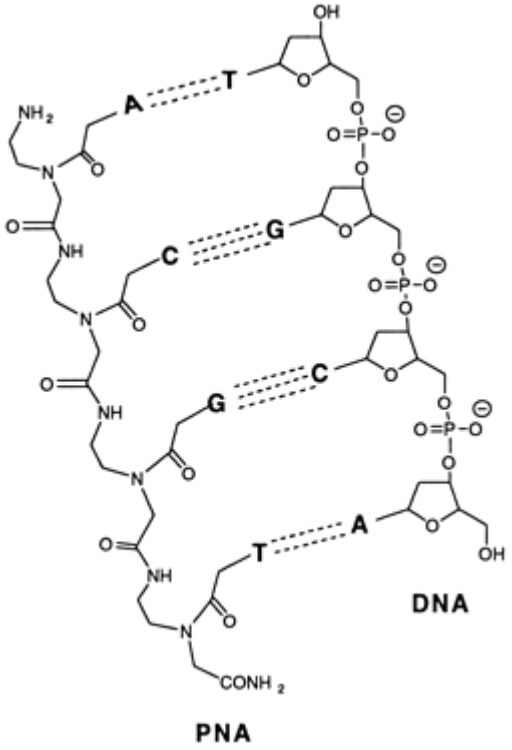

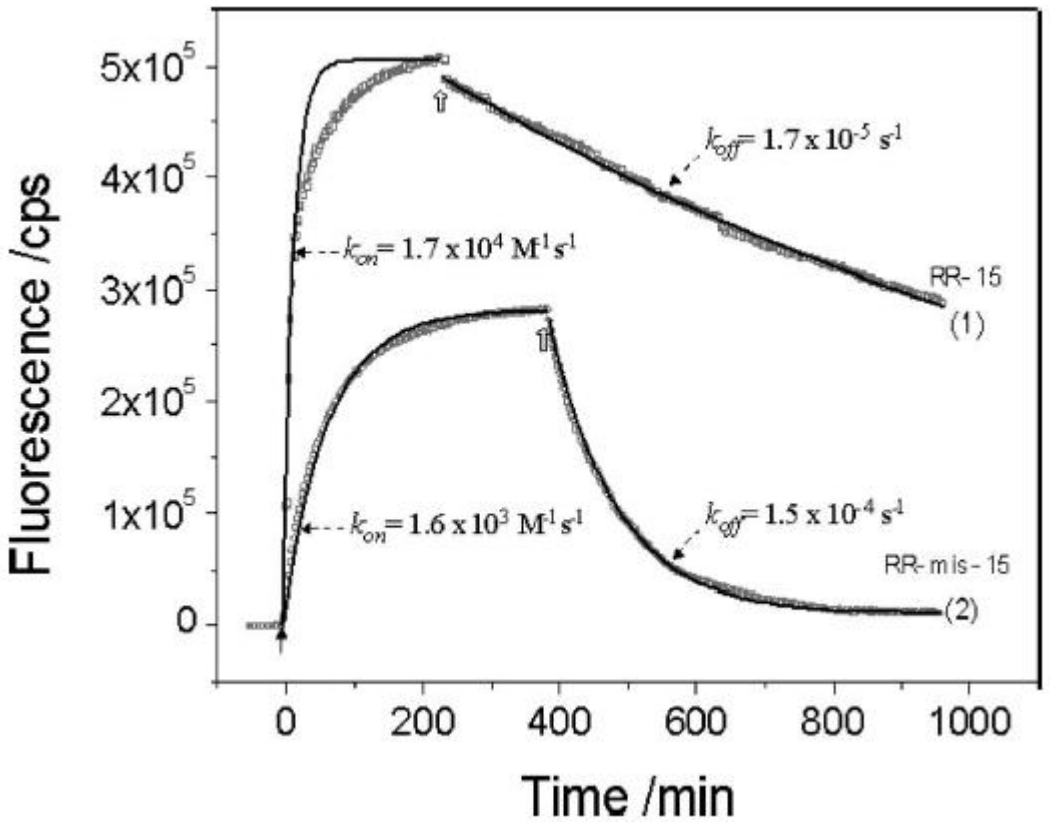

PNA probe: Biotin -AEEA -AEEA -TGCTAGAGTCAGCTT -NH_2

DNA targets:

RR-15	Cy5 –5’	AAGCTGACTCTAGCA-3'
RR- mis-15 [a]	Cy5 –5’	AAGCTGĞCTCTAGCA-3'

H. Park, A. Germini, S. Sforza, R. Corradini, R. Marchelli, and Knoll W. ,BioInterphases **1, 113 2006.**

EUROPEAN UNION
European Structural and Investment Funds
Operational Programme Research, Development and Education
MINISTRY OF EDUCATION, YOUTH AND SPORTS
FZU Institute of Physics of the Czech Academy of Sciences
AIT AUSTRIAN INSTITUTE OF TECHNOLOGY

Fitting of the Sensor Kinetics

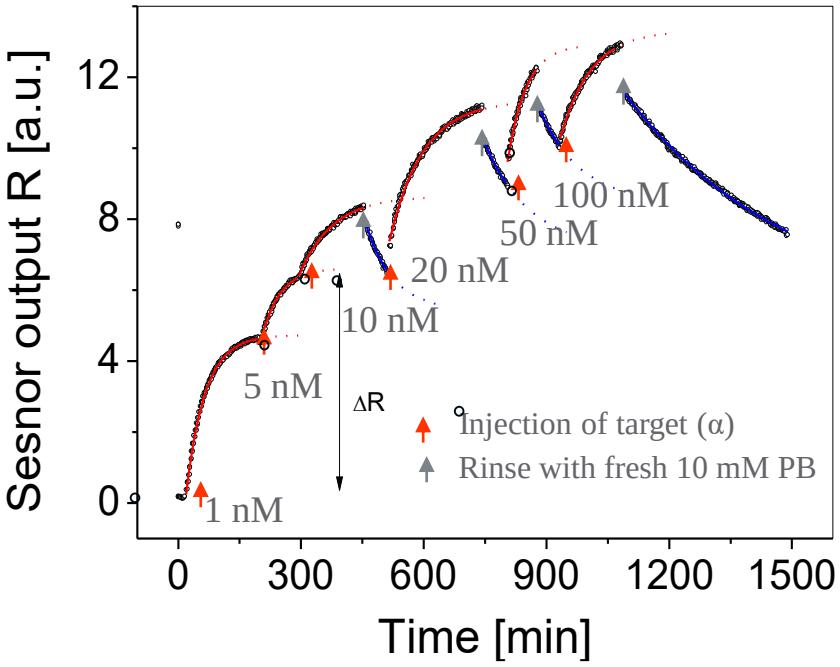

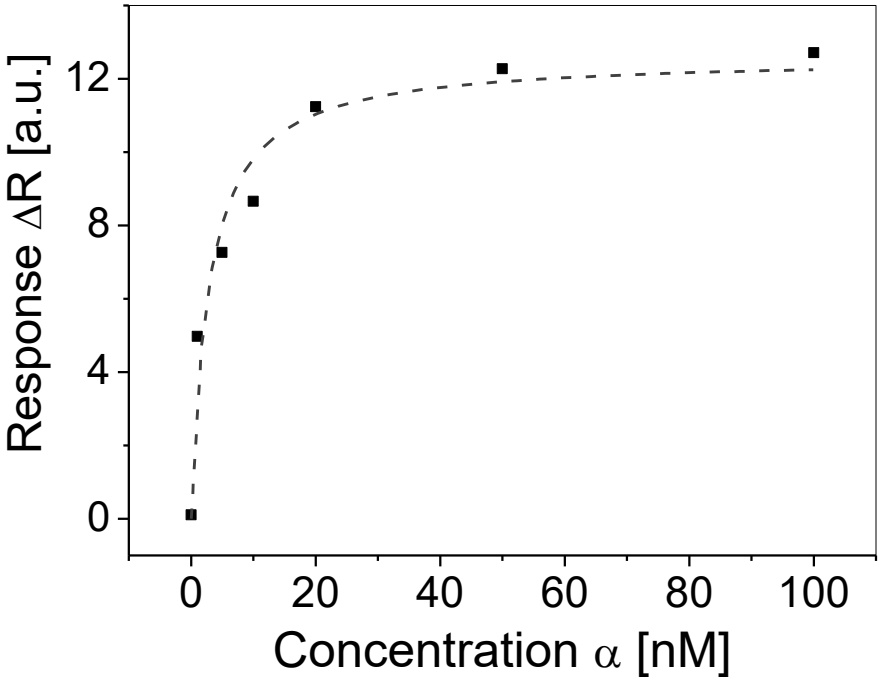

- By fitting the dependence of equilibrium sensor response *R* on the analyte concentration α the association affinity constant K_A can be fitted from a function:

$$\Delta R = const \frac{K\alpha}{1+K\alpha}$$

$$K_A = \frac{k_a}{k_d}$$

Global Analysis

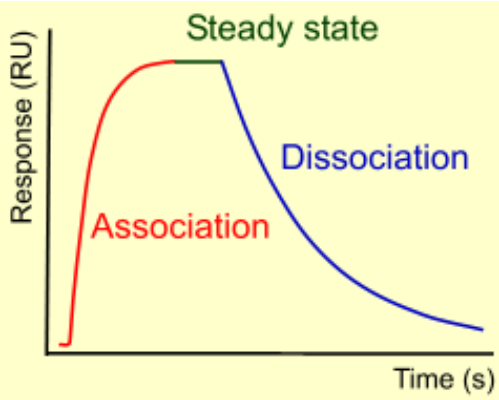

Fitting ⬇ kinetics

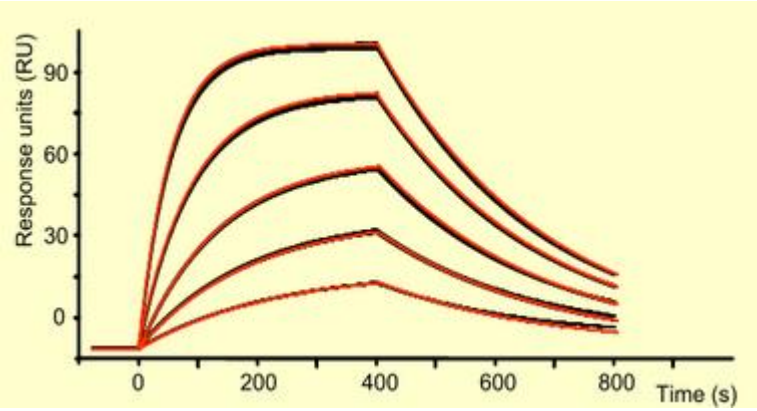

- Association and dissociation binding rates (k_a and k_d, respectively) or more complex parameters can be determined by fitting with a model.
- Analysis can be performed through specialized software (*e.g.* from BIAcore, Scrubber) or by another tools allowing fitting with non-linear functions (*e.g.* Origin).

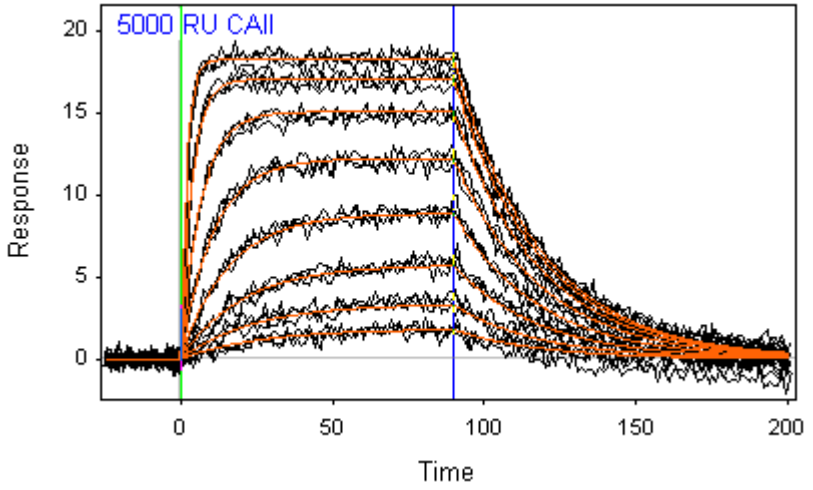

http://www.biologic.com.au/scrubber.html

Example of Non-Langmuir Kinetics

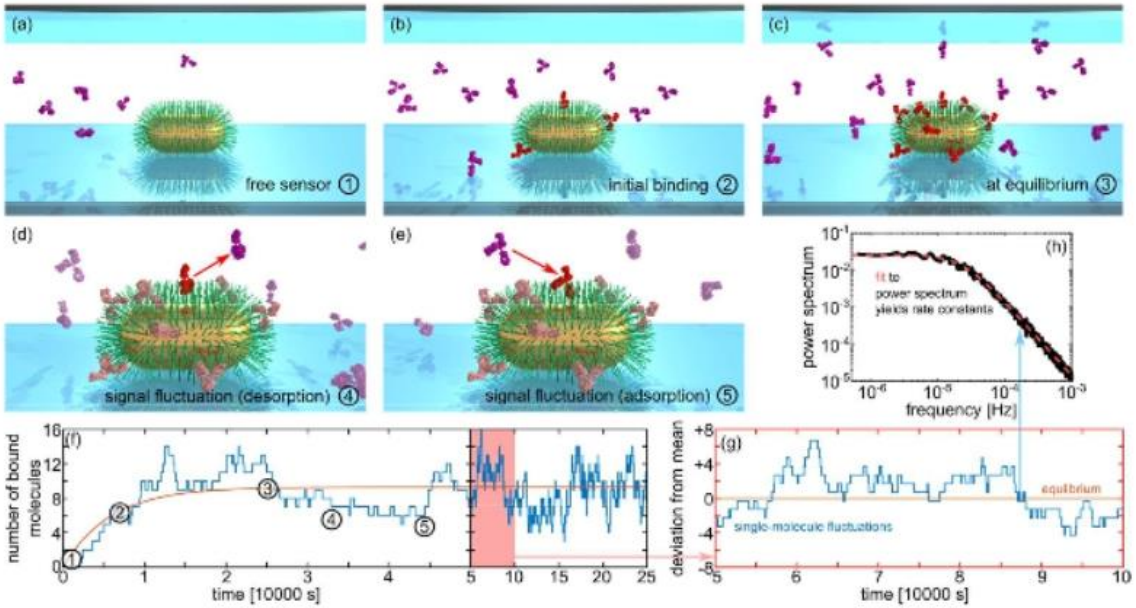

10.1021/acsnano.8b0401

Figure 1. (a-e) Nanoplasmonic LSPR sensing of single-molecule equilibrium fluctuations. (f) Simulated response of a nanosensor to binding of analyte molecules (blue) and the corresponding average over many sensors (orange). ① A nanorod covered with a receptor layer is exposed to flow of analyte solution. ② Analyte molecules bind to the receptors and surface coverage eventually reaches equilibrium ③, at which time-averaged numbers of associating and dissociating molecules are equal. However, molecules continue to ④ dissociate and ⑤ associate at random times. This causes short-time-scale fluctuations of the surface occupancy around the mean. (g) Once equilibrium is reached, molecules associate and dissociate stochastically with rates determined by k_{on}, k_{off}, and ρ, causing single-molecule fluctuations around the equilibrium signal. In this regime the system ceases to be mass transport limited. (h) Analysis of power spectrum of equilibrium fluctuations yields accurate values of rate constants.

Example of Non-Langmuir Kinetics

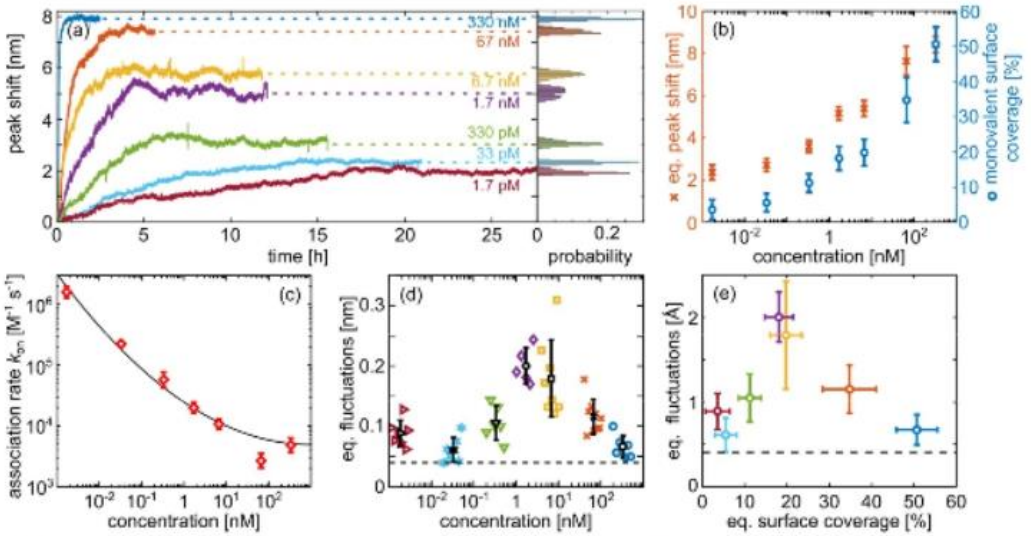

10.1021/acsnano.8b0401

Figure 3. (a) Exemplary Anti-PEG binding time traces for concentration between 330 nM and 1.7 pM and with at least 2 h of equilibrium fluctuations. The corresponding means are marked by dashed lines. The histograms visualize the span of observed peak variability with the largest widths for 6.7 and 1.7 nM. The equilibrium signal width is the smallest for the lowest and for the highest concentrations and increases toward the middle of the concentration range. (b) Equilibrium peak shift *vs* concentration. Red crosses denote absolute positions and blue circles estimated monovalent surface coverage. (c) Association rate constant (markers) obtained from fitting the kinetic adsorption curves using a bivalent analyte model (see SI) and interpolated dependence for simulations (solid line). Note, that for a large concentration range $k_{on}(\rho)$ is linear in the log-log scale indicating a power-law-like dependence. This is typical for hierarchical systems and agrees qualitatively with the association dynamics of Anti-PEG, which during binding enters partially the PEG brush necessitating the latter's rearrangement over the surface of the nanorod. (d) Amplitude of equilibrium fluctuations *vs* concentration. The individual colored symbols (artificial horizontal offset for clarity) mark values for individual traces and black ones corresponding averages. The dashed line marks the average magnitude of fluctuations before adding antibodies. (e) Equilibrium fluctuations *vs* equilibrium peak shift. The colors in panel (e) correspond to those in panel (d). The equilibrium fluctuations have the largest amplitude at *ca.* 20% surface coverage, while for both low and high values tend to the baseline fluctuations.

Force Measurements - k_d

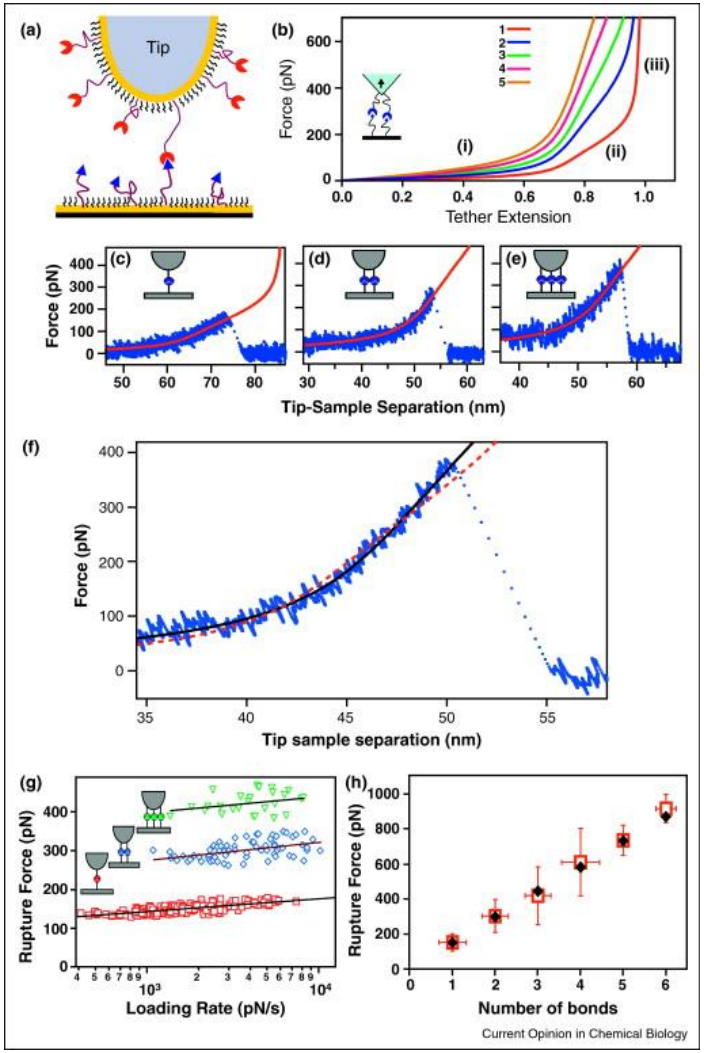

- AFM used for studying of force-induced disruption of affinity bound biomolecules, molecular stretching etc.

- $k_d=k_{d0}\exp(\gamma F/k_bT)$, where k_{d0} is the unperturbed dissociation binding rate, γ is the characteristic interaction length, F is the applied force and k_bT=4 pN·nm for the room temperature Assuming an interaction length γ of several nanometers.

T.A. Sulchek, R.W. Friddle, K. Langry, E.Y. Lau, H. Albrecht, T.V. Ratto, S.J. DeNardo, M.E. Colvin, A. Noy**Dynamic force spectroscopy of parallel individual Mucin1-antibody bonds** Proc Natl Acad Sci U S A, 102 (2005), pp. 16638-16643

Microfluidics

Lab-On-Chip and Micro-Total-Analysis-Systems

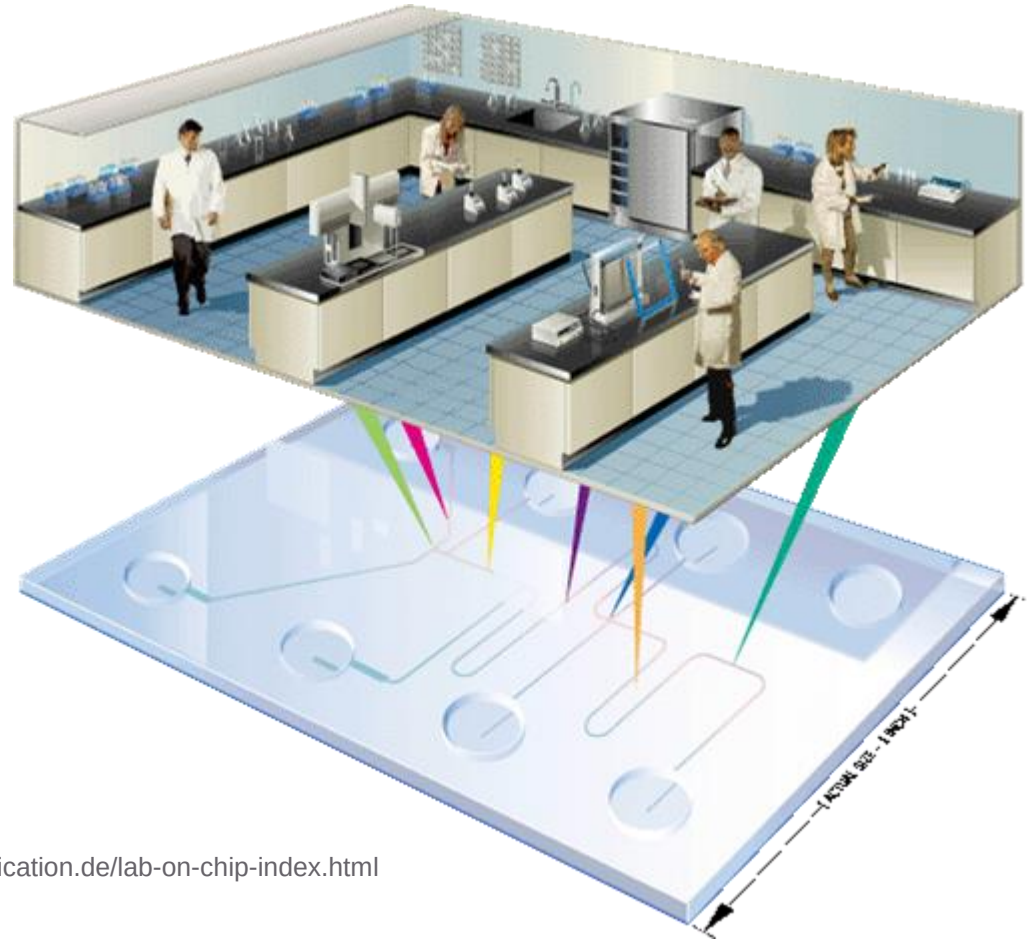

https://www.gene-quantification.de/lab-on-chip-index.html

Laminar Flow

- *Laminar flow:* viscosity-related effects are more important than inertial ones.
- Fluids mix only *via* diffusion, which is slow mechanism and makes reactions.
- Reynolds number Re<<1

$$Re = \frac{\rho u L}{\mu}$$

Re = reynolds number
ρ = density of the fluid
u = flow speed
L = characteristic linear dimension
μ = dynamic viscosity of the fluid

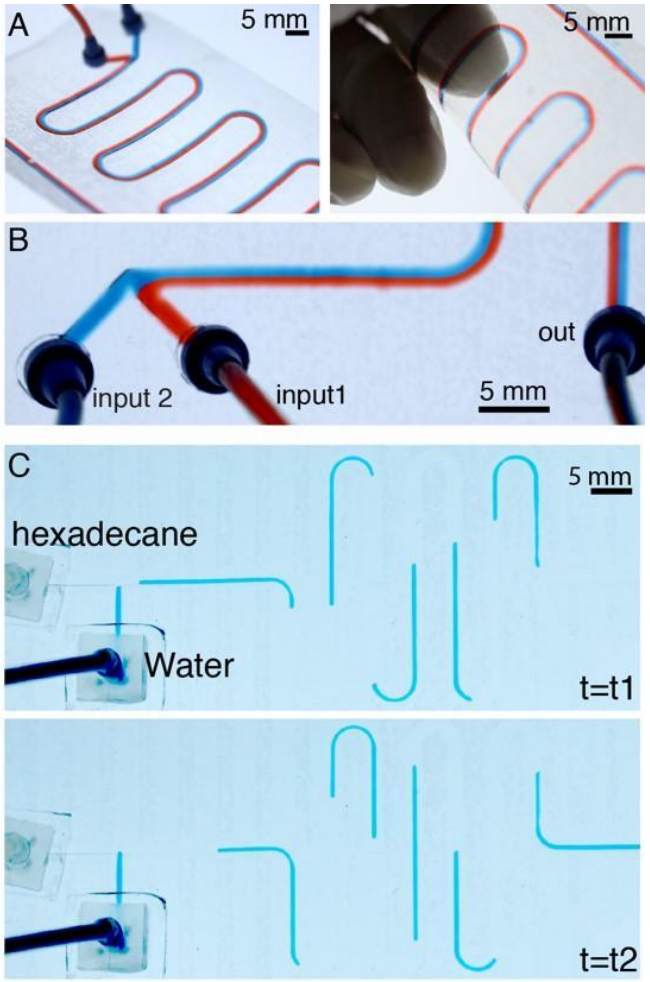

https://gmwgroup.harvard.edu/microfluidics

Laminar vs. Turbulent Flow

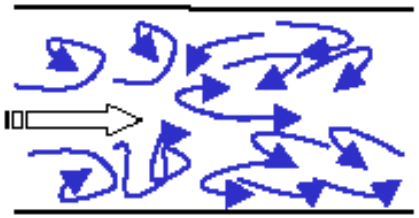

turbulent flow
unstable streamlines

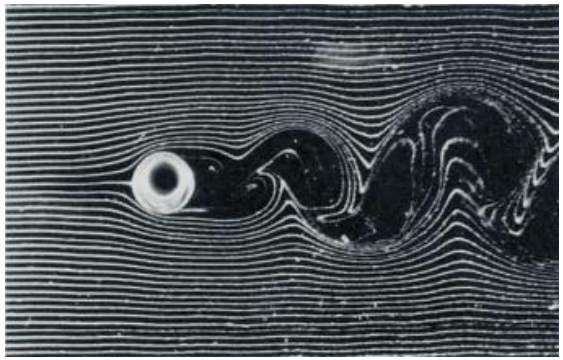

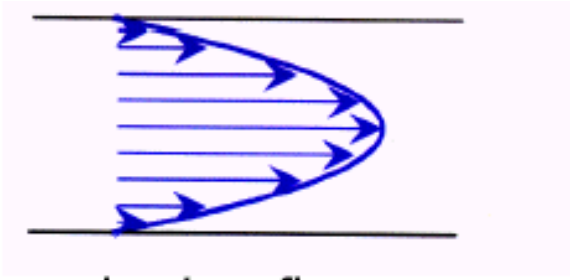

laminar flow
well-defined streamlines

Microfluidic Micromixers

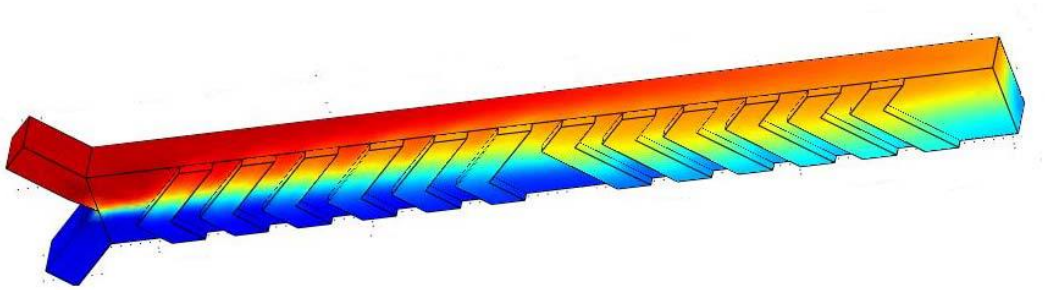

10.1109/SENSOR.2009.5285475

- Herringbone micromixer – texture introduced to flow channel wall that enable to speed up reaction limited by diffusion.
- The flow is still laminar, based on mixing that modify the regular parabolic flow velocity profile

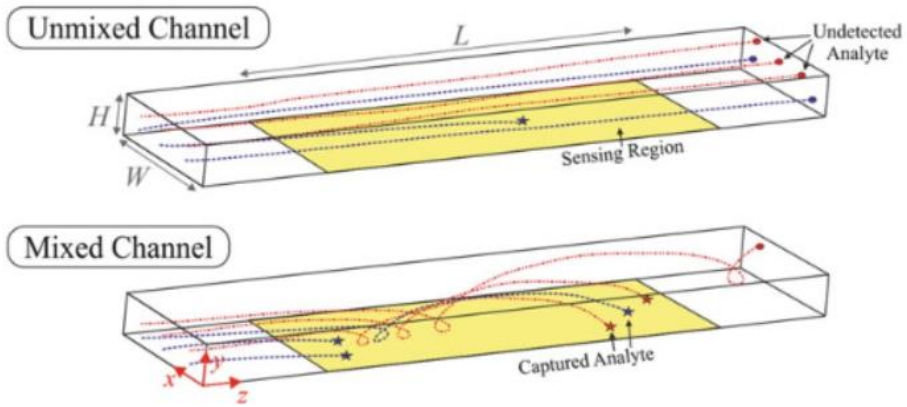

Fig. 1 The uniaxial flow in microfluidic channels often leads to a large percentage of analyte that does not interact with the sensing surface. The inclusion of mixing can increase the efficiency of analyte capture

https://doi.org/10.1007/978-3-319-64747-0_3

Microfluidic Micromixers

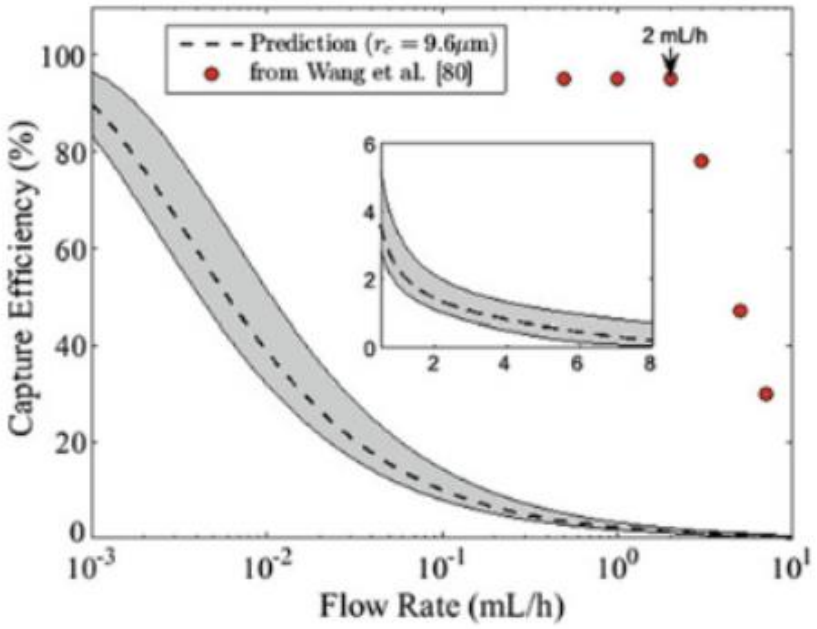

Fig. 12 Comparison of the data in [80]. SHM dimensions were reported as $W = 1$ mm, $H = 100\,\mu m$, $L = 880$ mm, $h_g = 35\,\mu m$, $w_g = 35\,\mu m$, and $\Lambda = 100\,\mu m$. The reported groove depth of $h_g/H = 0.35$ was used to estimate $U_t/U = 0.02$ [55], where we assumed $Sh_\infty = (PeU_tH/UW)^{1/3}$. Predictions of capture efficiency were calculated as $JLW/QCo \cdot 100$, where J was calculated using Eqs. (20)–(22). The dashed line pertains to predictions regarding cells of size $r_c = 9.6\,\mu m$. The upper and lower bounds of the shaded area pertain to cells of $r_c = 5.4$ and $13.8\,\mu m$, respectively. Diffusivities were calculated via the Einstein–Stokes relationship at 25C, where the viscosity of the DMEM medium was taken to be $\mu = 0.94$ cP [84]. Data representative of [80] is shown in the red symbols

https://doi.org/10.1007/978-3-319-64747-0_3

Diffusion-based Separation

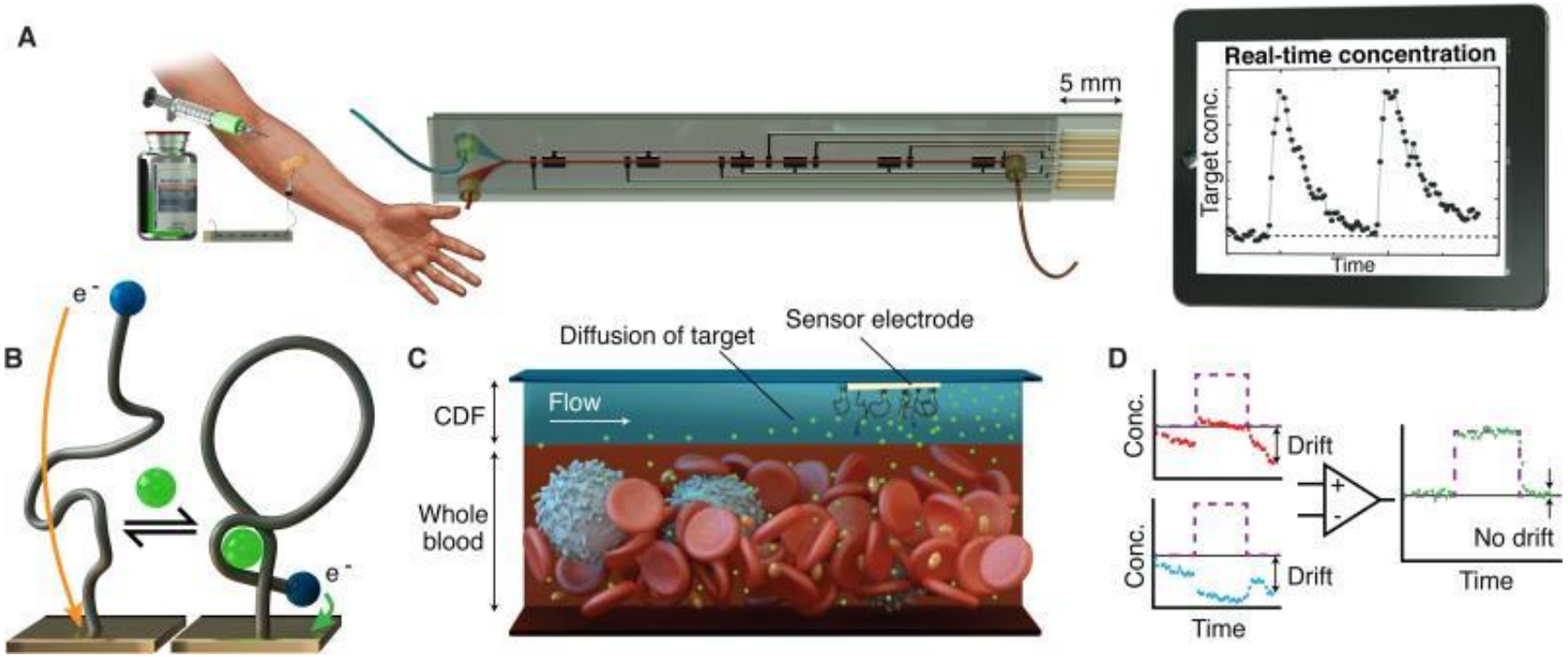

10.1126/scitranslmed.3007095

- Diffusion coefficient is dependent on the size of the molecules, can be used for separation of small molecules (e.g. therapeutic drug) from large molecules constituting blood (that would impair the sensor surface by fouling).

Assay Formats

Heterogeneous Assays

Direct/
Sandwich

Competitive

Inhibition

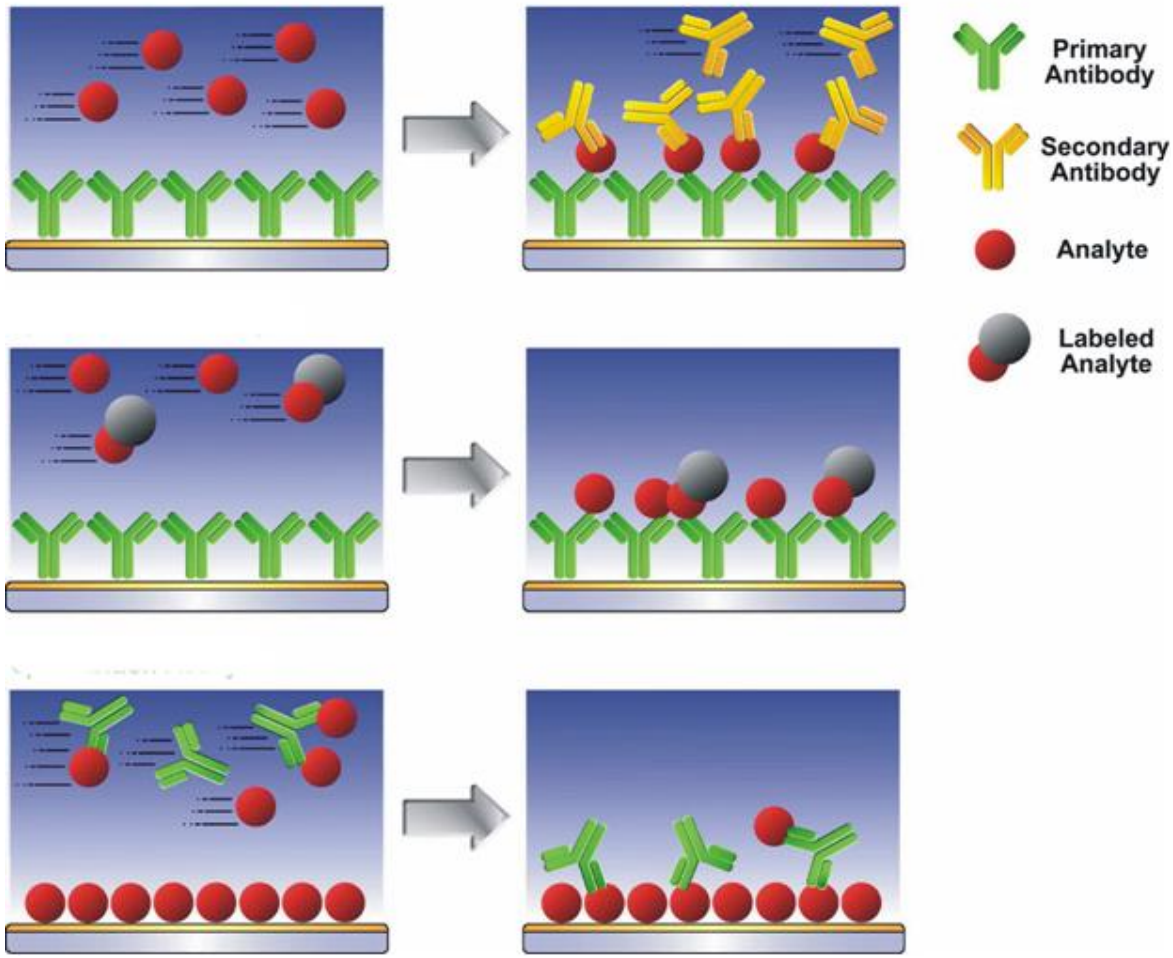

J. Homola (editor): Surface Plasmon Resonance Based Sensors, Springer, 2006.

Example of Direct Assay

Direct detection of luteinizing hormone (LH, triggers ovulation). Protein with molecular weight of 29 kDa.

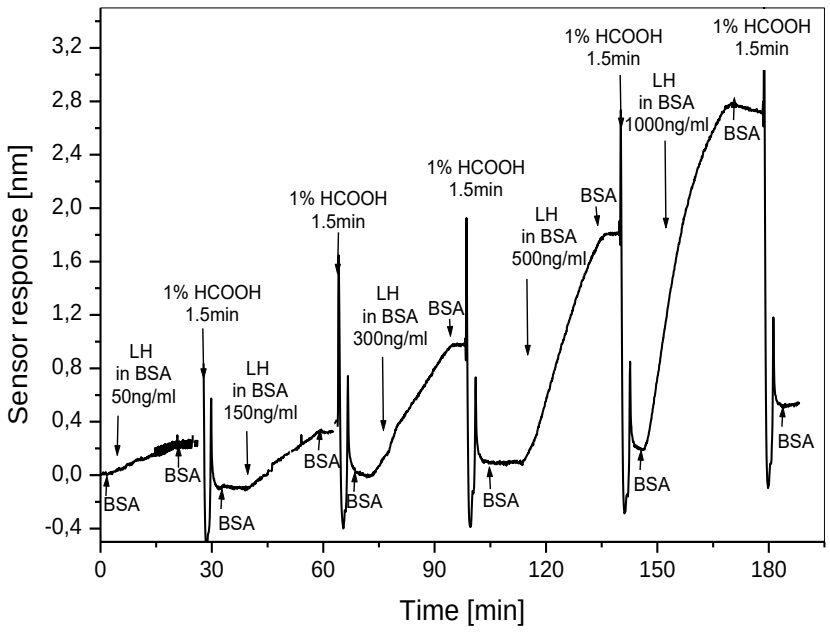

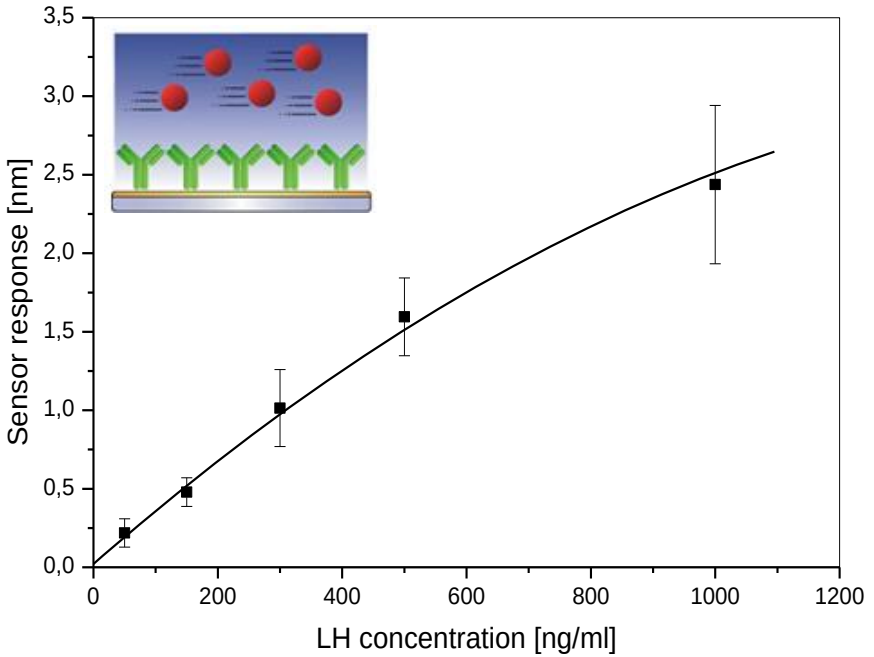

Binding kinetics for increasing concentrations of LH and regeneration between detection cycles (left) and the calibration curve (right).

Example of Sandwich Assay

Staphylococcal enterotoxin B (SEB) – toxin that commonly causes food poisoning, with severe diarrhea, nausea and intestinal cramping. Molecular weight 28 kDa. Response amplified by secondary polyclonal IgG with molecular weight of 160 kDa.

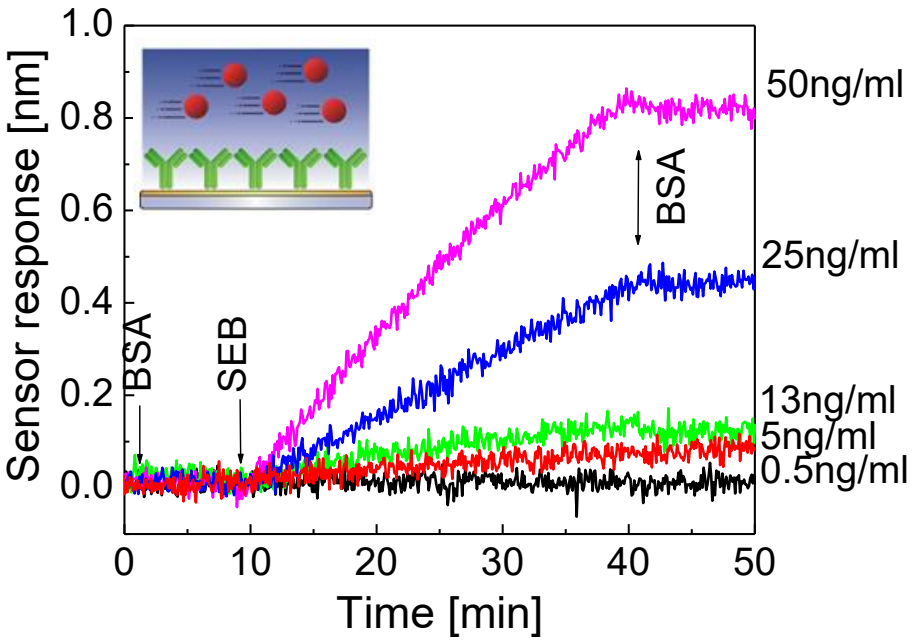

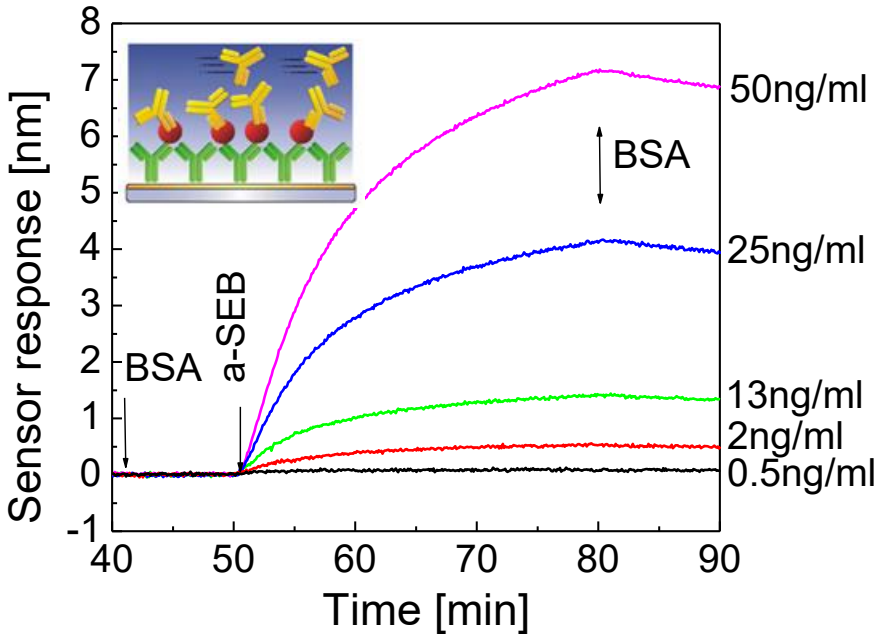

J. Homola, J. Dostalek, S. Chen, A. Rasooly, S. Jiang, S. S. Yee: Spectral Surface Plasmon Resonance Biosensor for Detection of Staphylococcal Enterotoxin B (SEB) in Milk , Journal of Microbiology, 75, (2002) 61-69.

Example of Inhibition Assay

Atrazine – pesticide with molecular weight of 0.2 kDa. Too small to be detected directly and thus inhibition or competitive assays are used.

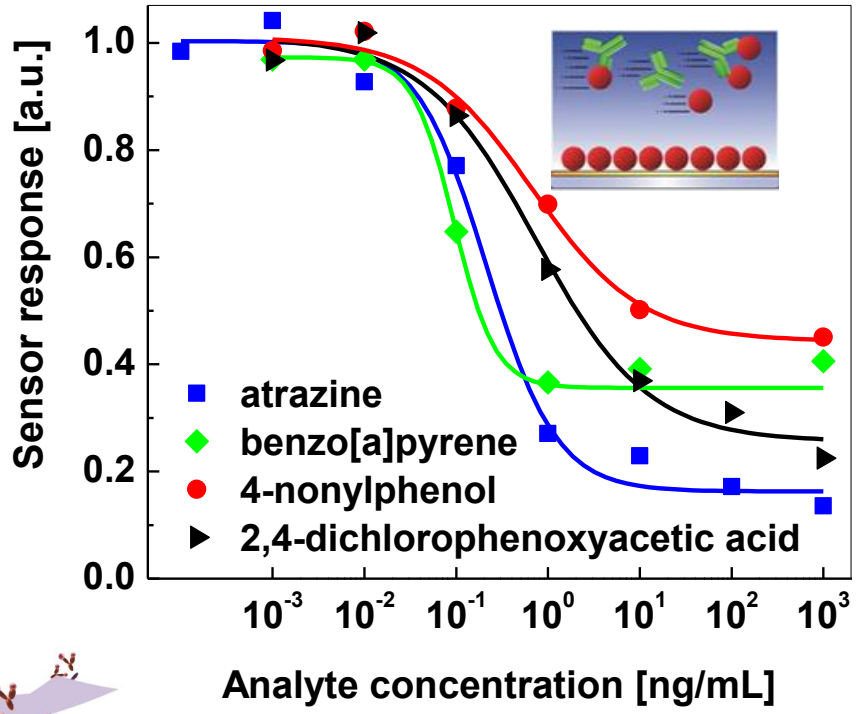

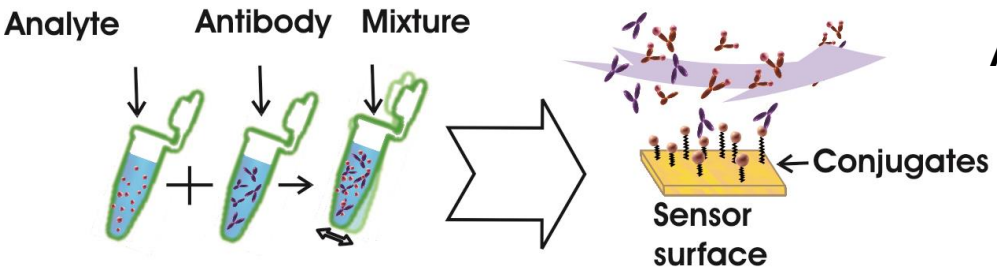

Dostalek, J. Pribyl, P. Skladal, J. Homola, Multichannel SPR biosensor for detection of endocrine disrupting compounds, Analytical and Bioanalytical Chemistry, (2007) 389:1841-1847